LETTER

High-Performance Single CdS Nanobelt Metal-Semiconductor Field-Effect Transistor-Based Photodetectors

Yu Ye, Lun Dai,* Xiaonan Wen, Peicai Wu, Ruomin Pen, and Guogang Qin*

State Key Lab for Mesoscopic Physics and School of Physics, Peking University, Beijing 100871, China

ABSTRACT We have demonstrated for the first time that under suitable gate biases, single CdS nanobelt (NB) metal-semiconductor field-effect transistors (MESFETs) can serve as high-performance photodetectors. When a gate voltage near to the threshold voltage of the MESFET under illumination is supplied, the single NB MESFET-based photodetectors exhibit high photosensitivity, such as ultrahigh photoresponse ratio ($I_{light}/I_{dark} \approx 2.7 \times 10^6$) (among the best values reported so far for single NB/NW photodetectors), high current responsivity ($\sim 2.0 \times 10^2$ A/W), high external quantum efficiency ($\sim 5.2 \times 10^2$), and fast photoresponse: with rise and decay times of ~137 and ~379 μs, respectively. The working principle of the single NB MESFET-based photodetectors as well as the reasons for the enhancement in performance is discussed. Our accomplishment can be easily extended to other 1D semiconductor nanomaterials. All the above results show that the single NB/nanowire (NW) MESFETs can be a promising candidate for novel photodetectors and photoelectronic switches.

KEYWORDS: photodetector • MESFET • nanobelts • CdS

INTRODUCTION

Semiconductor nanowires (NWs) or nanobelts (NBs), standing at the forefront of nanoscience and technology (1), have been studied extensively for potential applications in diverse nanosensors (2−6). Single NB/NW photodetectors may find applications as binary switches, lightwave communications, and optoelectronic circuits. So far, most of the reported single NB/NW photodetectors are two-terminal devices (2, 7−18). In general, for this type of photodetectors, there exists a trade-off among the performance parameters, such as current responsivity (R_λ), photoresponse ratio (I_{light}/I_{dark}), and photoresponse time (rise and decay times) (19, 20). For example, Golberg et al. reported ohmic contact-based single CdS NB photodetectors with ultrahigh R_λ ($\sim 7.3 \times 10^4$ A/W) and fast response time (~20 μs of both rise and decay times); however, their I_{light}/I_{dark} was quite low (~6) (14); Wang et al. reported Schottky contact-based NW photodetectors (15, 16) with a higher I_{light}/I_{dark} (~1020); however, their response time was not satisfying (~320 ms of decay time) (16). For practical use, exploring new ways to develop single NB/NW photodetectors with an overall enhancement in the performance is still indispensable.

Cadmium sulfide (CdS), an important II−VI compound semiconductor with a wide direct bandgap of ~2.4 eV at room temperature, has long been considered as a prospective material for optoelectronic devices (7, 8, 14, 16−18, 21). In this work, we demonstrate novel high-performance single CdS NB metal-semiconductor field-effect transistor (MESFET)-based photodetectors. Compared to the reported two-terminal single NB/NW photodetectors, the single CdS NB

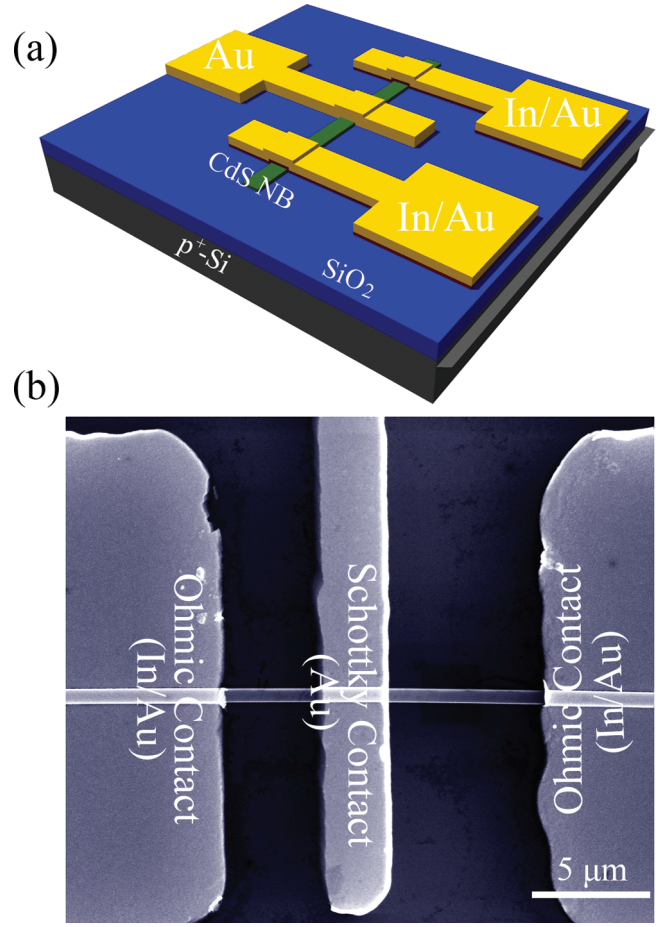

FIGURE 1. (a) Schematic illustration of a single CdS NB MESFET-based photodetector. (b) Typical FESEM image of a single CdS NB MESFET-based photodetector.

* Corresponding author. E-mail: lundai@pku.edu.cn (L.D.); qingg@pku.edu.cn (G.Q.).

Received for review July 28, 2010 and accepted October 6, 2010

DOI: 10.1021/am100661x

Published on Web 10/12/2010

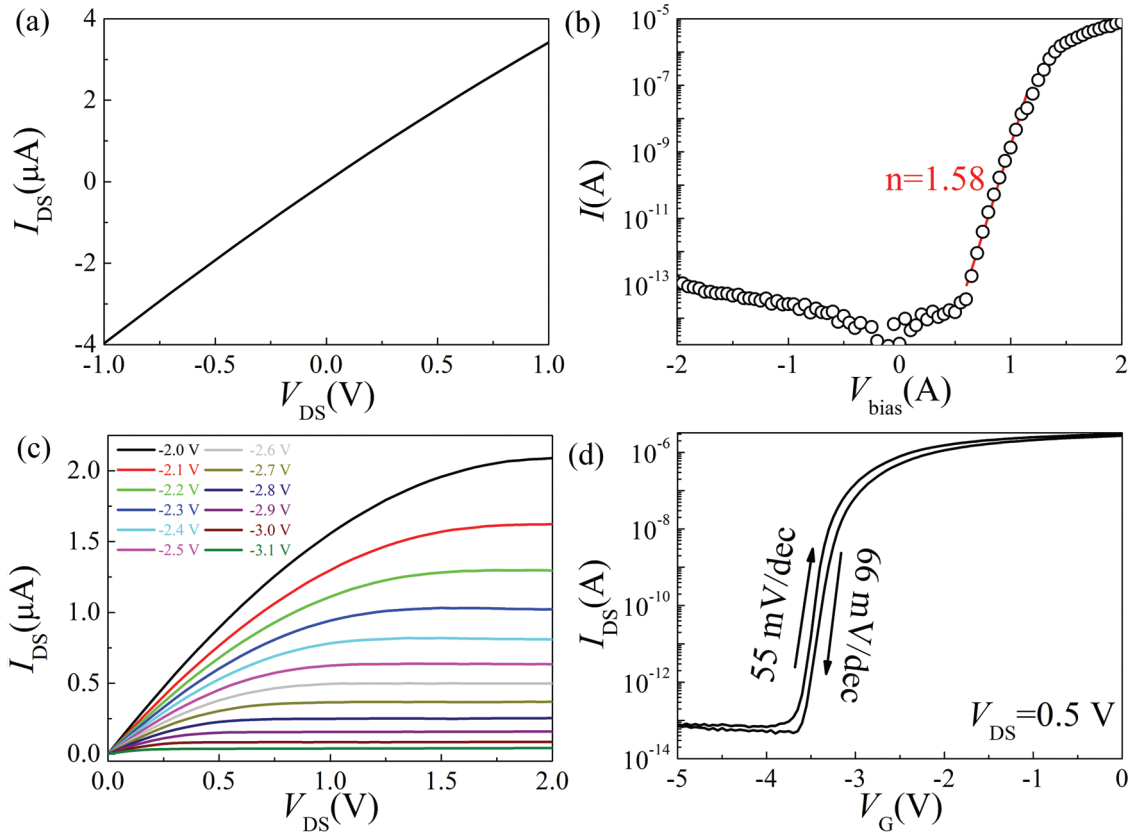

FIGURE 2. Typical electrical transport properties of the single CdS NB MESFETs. (a) $I-V$ curve measured between the source and drain electrodes at $V_G = 0$ V. (b) $I-V$ curve measured between the source and gate electrodes on an exponential scale. The red straight line shows the fitting result with the equation $\ln(I) = qV/nkT + \ln(I_0)$. (c) I_{DS} versus V_{DS} relations measured at various V_G (from −2.0 to −3.1 V). (d) I_{DS} versus V_G relations when the gate voltage was cycled between −5 to 0 V ($V_{DS} = 0.5$ V).

MESFET-based photodetector made a balance among overall performance parameters with the ultrahigh I_{light}/I_{dark} (~2.7 × 10^6), high current responsivity (R_λ~2.0 × 10^2 A/W), high external quantum efficiency (~5.2 × 10^2), and fast response (rise time ~137 μs; decay time ~379 μs). The as-fabricated MESFET-based photodetectors have the unique advantage of an additional dimensionality to control the channel conduction, and can be a promising candidate for the novel photodetectors and photoelectronic switches.

EXPERIMENTAL SECTION

The *n*-type CdS NBs used here were synthesized via the chemical vapor deposition method described previously (22). The device fabrication processes are as follows: First the CdS NBs were dispersed in ethanol with an ultrasonic process. Then the CdS NBs suspension solution was dropped onto an oxidized Si substrate with a 400 nm SiO_2 layer on the top. After that, two In/Au (10/100 nm) ohmic contact electrodes were defined on one single CdS NB with photolithography followed by thermal evaporation and lift-off process. Finally, one Au (100 nm) Schottky contact electrode was defined in between the ohmic electrodes across the CdS NB by similar process as mentioned above. Panels a and b in Figure 1 show a schematic illustration and a field-emission scanning electron microscope (FESEM) (FEI Strata DB 235) image of an as-fabricated photodetector, respectively. We can see that the NB has a uniform width (500 nm) along the entire length (13 μm) between the two ohmic contacts. Room-temperature electrical transport and photoresponse properties were characterized with a semiconductor characterization system (Keithley 4200) and a 200 MHz digital oscilloscope (Tektronix DPO2024). A 488 nm Ar^+ laser (Spectra-Physics 163C) was used as the light source.

RESULTS AND DISCUSSION

Typical electrical transport properties of the CdS NB MESFETs are shown in Figure 2. During the electrical transport measurements, the source electrodes were grounded. Figure 2a shows the $I-V$ curve measured between the source and drain electrodes. It shows a linear behavior, confirming the ohmic contacts between the In/Au electrodes and the CdS NB. Figure 2b shows the $I-V$ curve measured between the source and gate electrodes on an exponential scale. We can see a good Schottky contact rectification behavior between the Au electrode and the CdS NB. An on/off current ratio of ~1 × 10^8 is obtained when the voltage changes from +2 to −2 V. The turn-on voltage is around 1.25 V. The $I-V$ relationship of a Schottky junction can be expressed as $\ln(I) = qV/nkT + \ln(I_0)$, where q is the electronic charge, k is the Boltzmann constant, I_0 is the reverse-saturation current, and n is the ideality factor. For an ideal Schottky barrier, $n = 1$ (23). Here, by fitting the measured $I-V$ curve (the fitting result is shown with the red line in Figure 2b), we obtain $n = 1.58$. Figure 2c shows the source-drain current (I_{DS}) versus

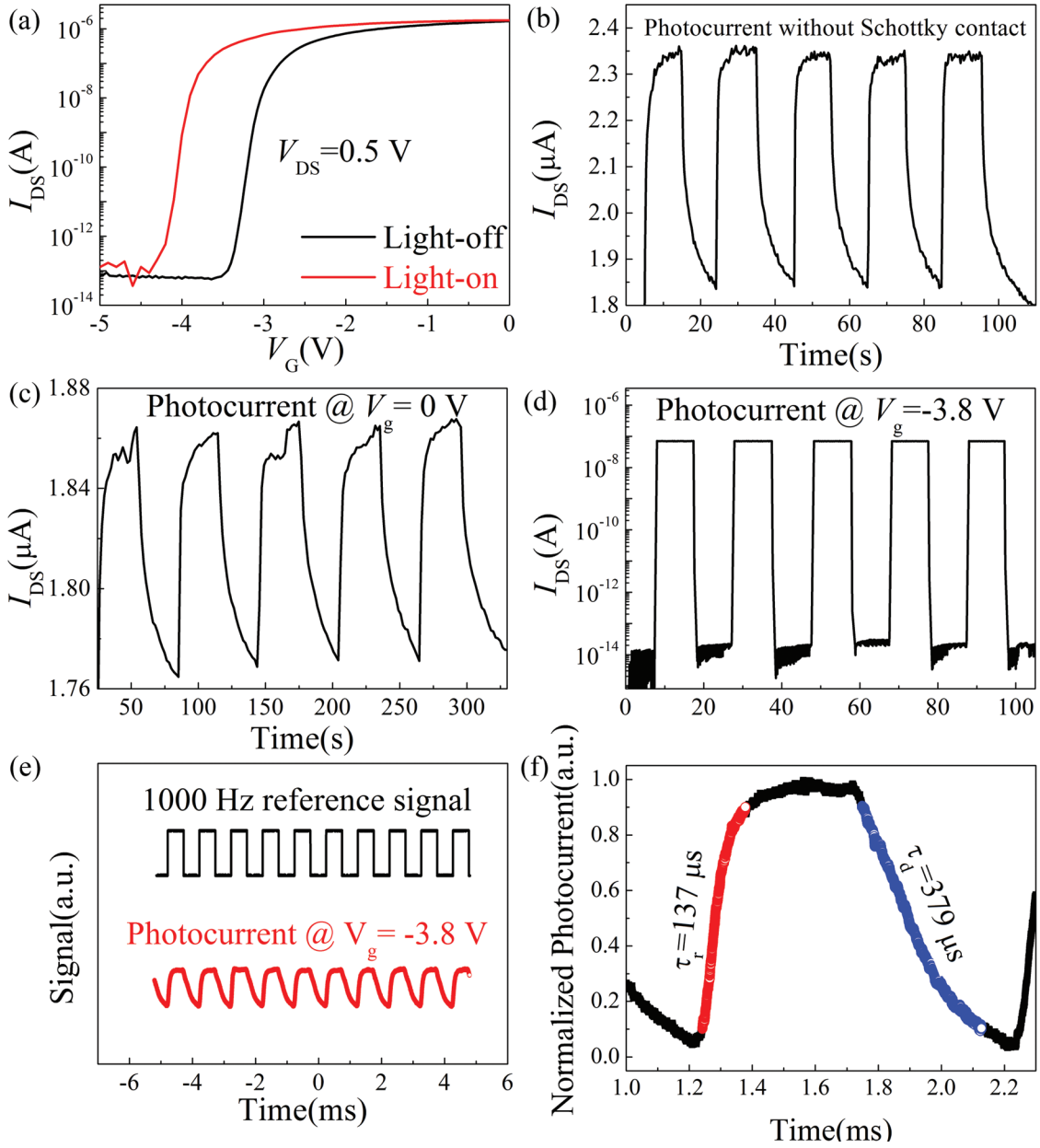

FIGURE 3. Typical light response properties of the single CdS NB MESFET based photodetectors. (a) Transfer characteristics of a CdS NB MESFET-based photodetector measured in dark (black line) and under illumination (red line). (b) On/off photocurrent response of the CdS NB without Schottky contact as a function of time. (c) On/off photocurrent response of the CdS NB MESFET-based photodetector with $V_G = 0$ V as a function of time on a linear scale. (d) On/off photocurrent response of the CdS NB MESFET-based photodetector with $V_G = -3.8$ V as a function of time on an exponential scale. (e) Transient response of the CdS NB MESFET-based photodetector (V_G=−3.8 V, $V_{DS} = 0.5$ V) along with a reference signal of the chopped light with a frequency of 1000 Hz. (f) Closeup of normalized photocurrent response in Figure 3e.

source-drain voltage (V_{DS}) relations measured at various gate voltages (V_G). For a given V_G, I_{DS} increases linearly with V_{DS} at lower V_{DS} and saturates at higher V_{DS}. Besides, the channel conductance shows a drastic decrease with applied negative V_G. Figure 2d shows the I_{DS} versus V_G relations when the V_G was cycled between −5 to 0 V. Only small hysteresis is observed. Besides, a large on/off current ratio (>10^7) and low subthreshold swings (S, 55 mV/dec and 66 mV/dec) can be obtained from Figure 2d. All these results demonstrate that the MESFET is of high performance.

The typical transfer characteristic curves of the CdS NB MESFETs with and without light illumination are depicted in Figure 3a. We can see that the V_{th} shifts from −2.9 to −3.8 V when the light is switched from off-state to on-state. This phenomenon can be understood as follows: there are two processes involved when the as-fabricated device is illuminated by photons with energy higher than the bandgap of CdS. One is that the channel conductance increases because of the photon-generated electrons and holes; the other is that photon-generated electrons and holes at the Schottky junction are separated by the strong local electric field (15, 24), which may reduce the electron−hole recombination rates, increase the free carrier density, and lower the barrier height (15, 16, 25). Both processes will make the CdS NB channel more difficult to be depleted, and hence the V_{th} shifts to a more negative value. The photocurrent response of a CdS NB without Schottky

contact as a function of time is shown in Figure 3b. We can see that it has a small photoresponse ratio ($I_{light}/I_{dark} \sim 1.27$) and a long decay tail (tens of seconds). Figure 3c shows the photocurrent response of the CdS NB MESFET as a function of time at $V_G = 0$ V. We can see that the average dark current (light-off) and photocurrent (light-on) are about 1.77 and 1.86 μA, respectively, resulting in an $I_{light}/I_{dark} \approx 1.05$. Again, long decay tail of tens of seconds can be observed.

Figure 3d shows the on/off photocurrent response of the CdS NB MESFET photodetector at $V_G = -3.8$ V, which is the threshold voltage of the MESFET under light illumination. We can see that the average dark current and photocurrent are about 26 fA and 70 nA, respectively, resulting in an I_{light}/I_{dark} as high as $\sim 2.7 \times 10^6$. To the best of our knowledge, this is so far among the highest reported values for single NB/NW photodetectors (7−18). In addition, the photoresponse processes (both rise and decay processes) are quite fast, which have exceeded the detection limit (0.3 s) of the measurement apparatus (Keithley 4200).

The current responsivity (R_λ), defined as the photocurrent generated per unit power of incident light on the effective illuminated area of a photoconductor, and the external quantum efficiency (EQE), defined as the number of electrons detected per incident photon, are two critical parameters for photodetectors. The large values of R_λ and EQE correspond to high sensitivity. The R_λ and EQE can be calculated with equations $R_\lambda = \Delta I/(P_\lambda S)$ and EQE $= hcR_\lambda/(e\lambda)$ (9), respectively. Here, ΔI is the difference between the photocurrent and the dark current, P_λ is the light power density, and S is the effective illuminated area, h is Planck's constant, c is the velocity of light, e is the electronic charge, and λ is the light wavelength. Using $\Delta I = 7.0 \times 10^{-8}$ A (measured from Figure 3d), $P_\lambda = 5.3$ mW/cm^2, $S = 500$ nm $\times 13$ μm (the effective illuminated area of CdS NB between two ohmic contacts measured from Figure 1b), $\lambda = 488$ nm, the R_λ and EQE of the CdS NB MESFET photodetector can be estimated to be about 2.0×10^2 A/W and $\sim 5.2 \times 10^2$, respectively.

To further investigate the detailed photoresponse times of the single CdS NB MESFET photodetector, we employed a 200 MHz digital oscilloscope with a 10 MΩ impedance and an optical chopper working at a frequency of 1000 Hz. Figure 3e shows the transient response of the CdS NB MESFET-based photodetector. From a closeup of the measured result shown in Figure 3f, the rise time, defined as the time needed for the photocurrent to increase from 10% I_{peak} to 90% I_{peak}, is 137 μs and the decay time, defined analogously, is 379 μs.

We attribute the overall high performance (e.g., the ultrahigh I_{light}/I_{dark} value, the high R_λ and EQE values, and the fast photoresponse) of our CdS NB MESFET based photodetectors to the unique advantage of the MESFET structure. In this structure, a much lower dark current can be obtained when applying a gate voltage near to the threshold voltage under illumination. Because, a gate voltage near to the threshold voltage of the MESFET under light illumination, which is more negative than the threshold voltage of the MEFSET in dark, helps to deplete the channel carriers when the light is turned off. This will further inhibit the long decay tail and result in a fast response for the MESFET based photodetectors.

CONCLUSION

In summary, high-performance single CdS NB MESFET-based photodetectors have been fabricated and studied for the first time. Compared with the traditional two-terminal photodetector, the MESFET-based photodetector has an additional dimensionality for control of channel conduction, which has the advantages of greatly reducing the dark current and increasing the photoresponse. With this approach, an overall enhancement in the performance of the photodetector has been realized. Our results show that the single NB/NW MESFETs can be a promising candidate for the novel photodetectors and photoelectronic switches.

Acknowledgment. This work was supported by the National Natural Science Foundation of China (10774007, 10874011, 50732001), the National Basic Research Program of China (2006CB921607, 2007CB613402), and the Fundamental Research Funds for the Central Universities.

REFERENCES AND NOTES

(1) Lieber, C. M.; Wang, Z. L. *MRS Bull.* **2007**, *32*, 99–108.
(2) Kind, H.; Yan, H. Q.; Messer, B.; Law, M.; Yang, P. D. *Adv. Mater.* **2002**, *14*, 158–160.
(3) Chen, R. S.; Wang, S. W.; Lan, Z. H.; Tsai, J. T. H.; Wu, C. T.; Chen, L. C.; Chen, K. H.; Huang, Y. S.; Chen, C. C. *Small* **2008**, *4*, 925–929.
(4) Cao, Q.; Rogers, J. A. *Adv. Mater.* **2009**, *21*, 29–53.
(5) Zhou, Y.; Wang, L.; Wang, J.; Pei, J.; Cao, Y. *Adv. Mater.* **2008**, *20*, 3745–3749.
(6) Kung, S.-C.; van der veer, W. E.; Yang, F.; Donavan, K. C.; Penner, R. M. *Nano Lett.* **2010**, *10*, 1481–1485.
(7) Jie, J. S.; Zhang, W. J.; Jiang, Y.; Meng, X. M.; Li, Y. Q.; Lee, S. T. *Nano Lett.* **2006**, *6*, 1887–1892.
(8) Gao, T.; Li, Q. H.; Wang, T. H. *Appl. Phys. Lett.* **2005**, *86*, 173105.
(9) Zhai, T. Y.; Fang, X. S.; Liao, M. Y.; Xu, X. J.; Li, L.; Liu, B. D.; Koide, Y.; Ma, Y.; Yao, J. N.; Bando, Y.; Golberg, D. *ACS Nano* **2010**, *4*, 1596–1602.
(10) Jiang, Y.; Zhang, W. J.; Jie, J. S.; Meng, X. M.; Fan, X.; Lee, S. T. *Adv. Funct. Mater.* **2007**, 1795–1800.
(11) Fang, X. S.; Xiong, S. L.; Zhai, T. Y.; Bando, Y.; Liao, M. Y.; Gautam, U. K.; Koide, Y.; Zhang, X. G.; Qian, Y. T.; Golberg, D. *Adv. Mater.* **2009**, *21*, 5016–5021.
(12) Fang, X. S.; Bando, Y.; Liao, M. Y.; Gautam, U. K.; Zhi, C. Y.; Dierre, B.; Liu, B. D.; Zhai, T. Y.; Sekiguchi, T.; Koide, Y.; Golberg, D. *Adv. Mater.* **2009**, *21*, 2034–2039.
(13) Zhai, T. Y.; Liu, H. M.; Li, H. Q.; Fang, X. S.; Liao, M. Y.; Li, L.; Zhou, H. S.; Koide, Y.; Bando, Y.; Golberg, D. *Adv. Mater.* **2010**, *22*, 2547–2552.
(14) Li, L.; Wu, P. C.; Fang, X. S.; Zhai, T. Y.; Dai, L.; Liao, M. Y.; Koide, Y.; Wang, H. Q.; Bando, Y.; Golberg, D. *Adv. Mater.* **2010**, *22*, 3161–3165.
(15) Zhou, J.; Gu, Y. D.; Hu, Y. F.; Mai, W. J.; Yeh, P.-H.; Bao, G.; Sood, A. K.; Polla, D. L.; Wang, Z. L. *Appl. Phys. Lett.* **2009**, *94*, 191103.
(16) Wei, T.-Y.; Huang, C.-T.; Hansen, B. J.; Lin, Y.-F.; Chen, L.-J.; Lu, S.-Y.; Wang, Z. L. *Appl. Phys. Lett.* **2010**, *96*, 013508.
(17) Liu, Y. K.; Zhou, X. P.; Hou, D. D.; W. H. *J. Mater. Sci.* **2006**, *41*, 6492–6496.
(18) Li, Q. H.; Gao, T.; Wang, T. H. *Appl. Phys. Lett.* **2005**, *86*, 193109.
(19) Shen, G. Z.; Chen, D. *Recent Pat. Nanotechnol.* **2010**, *4*, 20–31.
(20) Hangarter, G. M.; Bangar, M.; Mulchandani, A.; Myung, N. V. *J. Mater. Chem.* **2010**, *20*, 3131–3140.
(21) Zhai, T. Y.; Fang, X. S.; Li, L.; Bando, Y.; Golberg, D. *Nanoscale* **2010**, *2*, 168–187.
(22) Wu, P. C.; Ma, R. M.; Liu, C.; Sun, T.; Ye, Y.; Dai, L. *J. Mater. Chem.* **2009**, *19*, 2125–2130.
(23) Sze, S. M.; Ng, K. K. *Physics of Semiconductor Devices*; John Wiley & Sons: Hoboken, NJ, 2007.
(24) Ye, Y.; Dai, L.; Wu, P. C.; Liu, C.; Sun, T.; Ma, R. M.; Qin, G. G. *Nanotechnology* **2009**, *20*, 375202.
(25) Jin, Y. Z.; Wang, J. P.; Sun, B. Q.; Blakesley, J. C.; Greenham, N. C. *Nano Lett.* **2008**, *8*, 1649–153.

AM100661X